Acoustic analysis methods for particle identification with superheated droplet detectors

M. Felizardo[1,], M. Reis[1], A. C. Fernandes[1], A. Kling[1], T. Morlat[1] and J.G. Marques[1]*

[1]C[2]TN, Instituto Superior Técnico, Universidade de Lisboa, E.N. 10 (km 139.7), 2695-066 Bobadela, LRS, Portugal

Abstract. A superheated droplet detector (SDD) consists of a uniform dispersion of over-expanded, micrometric-sized halocarbon droplets suspended in a hydrogenated gel, each droplet of which functions as a mini-bubble chamber. Energy deposition by irradiation nucleates the phase transition of the superheated droplets, generating millimetric-sized bubbles that are recorded acoustically. A simple pulse shape validation routine was developed in which each pulse is first amplitude demodulated and the decay constant then determined through an exponential fit. Despite this, low amplitude (< 3 mV) events embedded at naked eye in the noise level are not counted for calibration purposes with neutron and alpha sources. The solution found was to filter the data with a low band-pass filter in the region that the bubbles nucleate (typically from 450 to 750 Hz). After this, a peak finding algorithm to count all the events was implemented. The performance demonstrates better than a factor 40 reduction in noise and an extra factor 10 reduction with the filtering application. The lowering of noise and discovery of low signal amplitudes by the acoustic instrumentation and acoustic analysis permits a capability of discriminating nucleation events from acoustic backgrounds and radiation sources and, having a 95% confidence level on identifying and counting events in substantial data sets like in calibrations.

1 Introduction

A superheated droplet detector (SDD) [1] is a generic denomination for a class of commonly employed systems for the neutron threshold spectrometry [2]. These consist of suspensions of metastable droplets which vaporize into bubbles when they are nucleated by radiation [3,4]. They have been used in neutron dosimetry for over one decade [5]; assessment of neutron spectra is achieved by measuring the bubble nucleation rate for different detectors or different operating temperatures, which exhibit different threshold energies, and then translating these results into an energy spectrum. The threshold energy of each detector depends on the composition of the droplets, their operation temperature and pressure conditions.

The various superheated emulsions share the same principle for neutron spectrometry but have different manufacturing procedures and constitution (either polymeric or aqueous gels) and also require different instrumentation for the bubble nucleation detection or counting. This has given rise to two different approaches for the measurement of the energy spectrum: the passive system which consists of six bubble (damage) detectors with energy thresholds ranging from 10 keV to 10 MeV, and the active system which uses superheated droplet detectors, usually one or two, which are operated at different temperatures to generate nested threshold responses in the 0,01-10 MeV range [6]. When using the passive detector system, which is also called the bubble detector spectrometer (BDS), the counting of the bubbles is done optically at the end of the irradiations, either by eye or by means of an automated camera procedure. In the case of the active system, also referred to as the bubble interactive neutron spectrometer (BINS), the bubbles are counted acoustically in real time by detecting the pressure pulses emitted when they suddenly vaporize. This will be the one we will be interested in henceforth.

In this paper, we investigate their response to low energy alpha particles (α) during temperature ramping.

The response of SDDs to α irradiations has been previously studied in Refs. [7,8], mostly however using either a uranium composite (U_3O_8) or ^{241}Am distributed in the gel matrix; the response to ^{226}Ra at various temperatures was examined in Ref. [9], and use of an external source was reported [10] using small CCl_2F_2 droplet sizes (3±1μm). The response of superheated C_4F_{10} emulsions to alpha particles has been studied [11] by simulation using the GEANT3.21 toolkit, with the alpha contamination present either in polymer or both the polymer and active liquid.

The focus of this study was on the SDD response to α-emitting elements (in preparation): uranium and samarium with dominating energies E_α of 4722 and 4774 keV for ^{234}U, 4151 and 4198 keV for ^{238}U as well as 2248 keV for ^{147}Sm. The contribution from α-decays of other natural isotopes can be neglected due to low natural abundance (^{235}U) or significantly longer half-lives (^{148}Sm, ^{149}Sm), using devices containing small diameter (~ 5 μm) C_2ClF_5 droplets. The experimental set-up for the study is described in Sec. 2. The instrumentation employed is described in Sec. 3.The acoustic analysis and methodology are discussed in Sec. 4. Results of the better performance of identifying and validating nucleation events are shown in Sec. 5. Finally, conclusions are drawn out in Sec. 6.

Detector physics and production

We will not delve deeply into the physics behind the SDD operation, but we do feel it useful, for clarification purposes, to include a short description and make explicit the composition of the detectors used in our experimental essays.

Superheated emulsions share the working principle with bubble chambers, commonly used in high-energy particle physics and dark matter searches, where each droplet acts as a mini-bubble chamber. One important difference lies in the fact that the superheated emulsions are continuously sensitive since the liquid is kept in steady-state superheated conditions, i.e., above its boiling point, whereas in the bubble chamber the liquid is only sensitized for brief periods of time. When a heavy charged particle slows down in moving through the liquid, kinetic energy is transferred as thermal energy generating trails of sub microscopic vapour cavities inside the droplets, which induce an expansion of the bubble

and eventually its evaporation. The amount of energy and the critical size required for bubble nucleation depends on the composition and on the degree of superheat of an emulsion. Typically, the higher the superheat of the droplets, the lower is the nucleation energy required for their evaporation, i.e., the lower is the threshold energy of the detector.

The detector gel was prepared by combining 4.9 g gelatin + 19.5 g of bi-distilled water (bdw), and melting at 60 °C for 20 min; separately, 10g of PolyVinylPyrrolidone (PVP) + 24.9 g of bdw were combined and also melted at 60 °C for 20 min. The gelatin and PVP solutions were then blended for 20 min at 60 °C, and 50.8 g of the concentrated gel added to 185.5 g of glycerin in a 150 ml bottle and heated at 80 °C for 1h30 with slow agitation. The hot gel was outgassed, a necessarily step to remove all air trapped during the fabrication process: measurements showed that without outgassing, the response was flat [12].

A quantity of radioactive liquid source was then injected within the hot gel at 44 °C and agitated quickly before being placed inside the hyperbaric chamber. For the U solution (Uranium Standard solution in HNO_3 2-5% U =1.000 g/l ICP), the quantities were: 30 µl (0.37 Bq) and 300 µl (3.7 Bq); for the Sm (Sm_2O_3 in 5% HNO_3; Sm=10^4 µg/ml), 600 µl (0.37 Bq). To verify the actual α emission spectra from Uranium and verify sources activities, the α spectrum of the U source was measured by α-spectrometer; the measured element concentration agreed with the nominal value within ±4%. Two radioisotopes were identified, ^{234}U and ^{238}U, with the same activity, indicating that the two isotopes were in equilibrium and leading to the emission of four α's (^{234}U: {4774keV at 71%; 4722keV at 28%} and^{238}U: {4198keV at 79%; 4151keV at 21%}); the emission from ^{235}U was negligible. In case of Sm, only one α (2248keV at 100%) was present, from the isotope ^{147}Sm.

The emulsion fabrication was made at 44°C at 20 bar for 4 h, with a stirring at 300 rpm. The temperature was then stopped for 1 h and the agitation slowed to 50 rpm. An hour later, the emulsion was cooled by cold water circulation at 5°C for 12 hours, the pressure then slowly released and the SDD extracted for use.

2 Experimental Set-up

Each SDD was placed inside a temperature-controlled, circulating water bath, surrounded by a radiation shielding (1 m x 0.8 m x 0.75 cm) made of concrete blocks (40 cm height) topped by paraffin (30 cm height) and polyethylene (1 m x 0.8 m x 0.05 m). Inside the shielding a 5 cm acoustic foam was installed to reduce the ambient noise (without acoustic foam, only events with amplitudes higher than 2 mV were detected; with acoustic foam, events with amplitudes lower than 0.4 mV could be detected). The bath temperature was monitored with an un-doped SDD containing a temperature probe.

The SDD signals were measured in atmospheric pressure at temperatures in steps of 1ºC between 5 – 13°C (above 13°C, γ-ray nucleation sensitivity begins) for two activities of U and for 0.3 Bq of Sm. The time required for thermalisation between adjacent steps was of order 1-2h. After thermalisation signal acquisition started, taking from 20 min up to 1 h, depending on the event rate. The non-spiked SDD was used for background measurements [13,14].

3 Instrumentation

The acoustic instrumentation employed was the same as the one used in the SIMPLE experiment [15,16].

The DAQ system records the acoustic wave associated with the rapid bubble expansion following a nucleation event, and consists of a high quality electret microphone cartridge (MCE-200) with a frequency range of 20 Hz – 16 kHz (3 dB), SNR of 58 dB and a sensitivity of 7.9 mV/Pa at 1 kHz. This is connected to a high gain, low noise and high flexibility digitally-controlled microphone preamplifier (PGA2500 from *Texas Instruments*), which is coupled to the input of an acquisition channel [13]. Data was acquired in *Matlab* files of ~ 15 MB each at a constant rate of 32 kSps for a period of 10 minutes each.

Mechanically the microphone, ensheathed in a protective latex covering, is installed inside the detector container within a glycerin layer above the droplet suspension, which serves as an excellent acoustic enhancer [17,18].

4 Acoustic Analysis and Methodology

Figure 1 shows a typical bubble nucleation event and its frequency spectrum obtained with a normal standard test device. The FFT is characterized by a peak at ~640 Hz, with some lower power harmonics around 2 and 4 kHz.

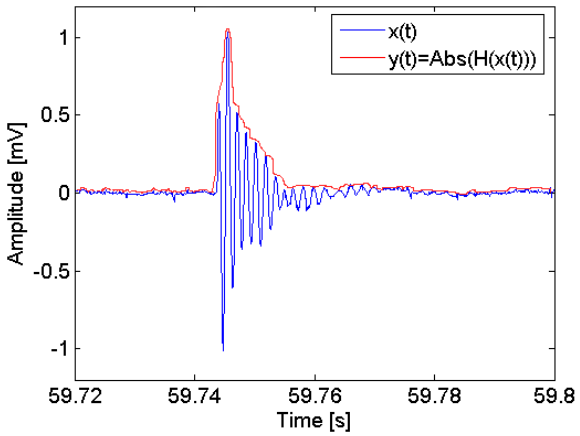

(a)

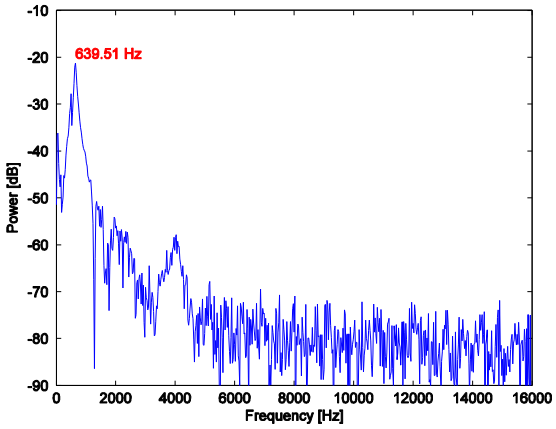

(b)

Fig. 1: Typical pulse shape (a) and its FFT (b) of a bubble nucleation event.

As in Ref. [7], the nucleation events were generally stimulated by environmental radiations. These were cross-checked against events generated by irradiating the detectors using a quasi-monochromatic 54 keV neutron beam obtained with a Si+S passive filter at the Portuguese Research Reactor [19].

As a first stage discrimination filter for distinguishing true nucleation events from acoustic backgrounds, a pulse shape validation routine [17] was adopted. This routine sets an amplitude threshold, identifies the beginning and end of each spike based on the previous threshold, amplitude-demodulates the time evolution of the spike, measures the decay time constant (τ) of the pulse and finally suppresses pulses exhibiting τ's below a selected threshold.

The choice of the amplitude threshold is an interactive procedure, and can be set very low for the rejection of spurious noise. Amplitude demodulation is achieved simply with the modulus of the Hilbert transform of the pulse waveform, $y(t) = |H\{x(t)\}|$. After the amplitude envelope has been obtained, the maximum and the minimum of the pulse shape are found to set the time window used for evaluating τ. The decaying part of the envelope is then fit to an exponential, $h(t) = Ae^{-t/\tau}$ by means of a linear regression after linearizing the envelope, $\ln(y(t)) = \ln(A) - t/\tau + er(t)$ where $er(t)$ corresponds to the residual of the fit. Figure 2 shows the decay interval of the envelope, and the exponential fit. An efficiency of ~97% at a 95% CL was obtained with a τ window of 10 -40 ms.

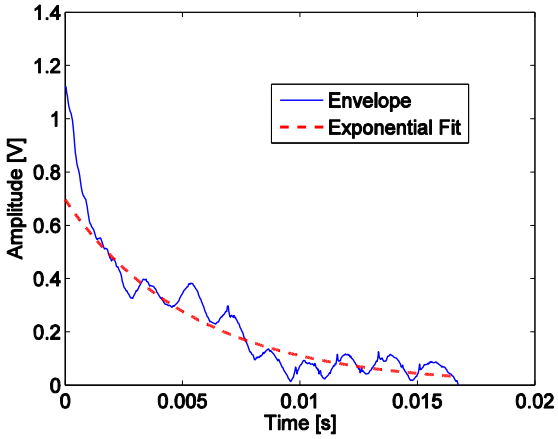

Fig. 2: Best fit to an exponential function of the amplitude envelope from the pulse shown in Fig. 1(a), with $\tau \sim 20$ ms.

In the case of α sources studies this has been much difficult to see, since the droplet sizes utilized are much smaller as said previously. As seen in Fig. 3, small events must be embedded in the noise level and with the acoustic routines of identification only 41 events are accounted for. Consequently, the interactive choice of this amplitude threshold is not optimized or valid for small droplet sizes. Accordingly, a new approach must be engaged.

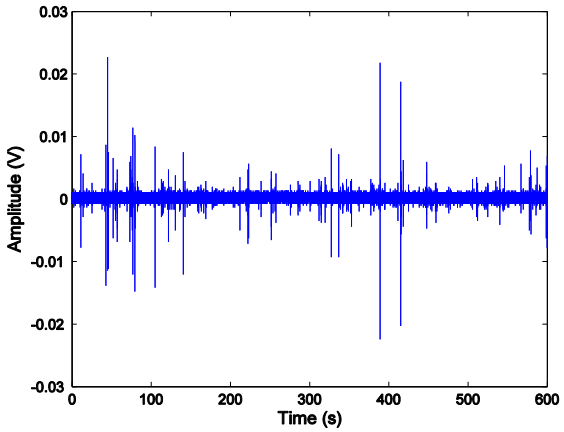

Fig. 3: Acoustic signal of 41 bubble nucleation events evaluated for a 10 minute α calibration run.

A common requirement in scientific data processing is to detect peaks in a signal and to measure their positions, heights, widths, and/or areas. One way to do this is to make use of the fact that the first derivative of a peak has a downward-going zero-crossing at the peak maximum. But the presence of random noise in a real experimental signal will cause many false zero-crossing simply due to the noise. To avoid this problem, the technique described here first smoothes the first derivative of the signal, before looking for downward-going zero-crossings, and then it takes only those zero crossings whose slope exceeds a certain

predetermined minimum (the "*slope threshold*") at a point where the original signal exceeds a certain minimum (the "*amplitude threshold*"). By carefully adjusting the smooth width, slope threshold, and amplitude threshold, it is possible to detect only the desired peaks and ignore peaks that are too small, too wide, or too narrow (events identified as noise or spurious events from gel defects, fractures, N^2 gas releases, etc). Moreover, this technique can be extended to estimate the position, height, and width of each peak by least-squares curve fitting of a segment of the *original unsmoothed signal* in the vicinity of the zero-crossing. Thus, even if heavy smoothing of the first derivative is necessary to provide reliable discrimination against noise peaks, the peak parameters extracted by curve fitting are not distorted by the smoothing, and the effect of random noise in the signal is reduced by curve fitting over multiple data points in the peak. This technique is capable of measuring peak positions and amplitude heights quite accurately. For the most accurate measurement of these peak shapes, or of highly overlapped peaks, or of peak superimposed on a baseline, that occur during massive calibrations, the related digital filters with selectable peak shape models and baseline correction modes provide an optimal tool together with the validation routines to perform true event accounting.

One more issue that one has to take into account is the signal attenuation by the increase of bubble nucleation in these immense calibration sets. Previous studies [20,21] have suggested an acoustic signal attenuation caused by the increasing bubble population. The presence of bubbles in a volume fraction of 0.4% has a substantial effect on its acoustic properties [20], and reduces the velocity of sound at low frequency to 0.2 mm/μs. In our case, a volume fraction of 0.4% suggested V = 0.4% x 150 ml = 0.6 ml; by assuming that all bubbles have a diameter of 1 mm, $V = 4/3N\pi <0.5\ mm>^3 = 0.6$ ml and N ~1150 bubbles: 10^3 bubbles inside an SED would be enough to cause attenuation of the sound amplitude. This suggests that these type of calibrations should not last longer than ~two hours.

5 Results

As said before, the final objective of these studies (in preparation) are not dealt with in this short paper, but the new discoveries (smaller droplet sizes used in α-doped SDDs) that generate to a great extent smaller amplitude nucleation events which, if not accounted for, will harm the final results of the SDDs behavior.

A review of the experiments noted that visual observations, before and after each run, yielded many bubbles than recorded by the microphone and estimated by the event count rate of the radiation source; the main frequency of the acoustic signal was observed to vary with temperature and the accumulated SDD exposure.

Assuming the methodology explained before, a simple and fast command-line function to locate and count the positive peaks in noisy data sets was performed. Together with the identification routines of the different characteristics that are used to identify events, permits an optimized improvement for validation of events, such as in dark matter searches. The fast command-line function detects: (1) peaks by looking for downward zero-crossings in the smoothed first derivative that exceed the *SlopeThreshold*, (2) peak amplitudes that exceed the *AmpThreshold* and, (3) returns a list (in a matrix) containing the peak number and the measured position and height of each peak.

Figure 3 indicates that many events were submerged in the background with its fixed frequency filtering; when the filter was re-tuned to a lower frequency window (100-300Hz), higher event rates were obtained which allowed extension and better agreement with what

was predicted of the SDD response. Despite this, to perform the amplitude peak analysis, an intermediate step was introduced to avoid false triggering due to spurious noise within the signals. This first-hand filtering pace uses the outlier-robust Hampel identifier to detect spikes and replaces them with the median value of local values. The impulsive noise spikes are removed as effectively as they are by the median filter, but the low-level detail preservation is much better. Like this, the new noise level is of 0.13 mV, which corresponds to a reduction of 47%. Figure 4 shows the result of this accomplishment (application of the band-pass filter and the outlier-robust Hampel identifier).

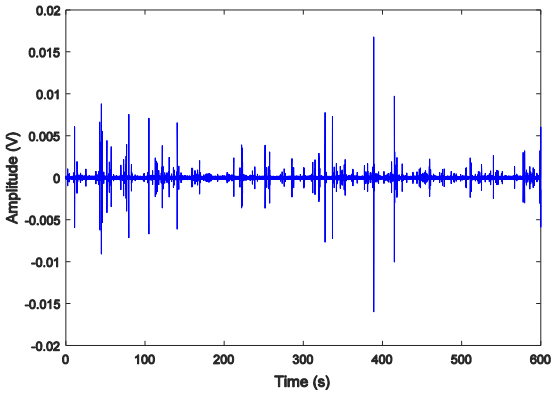

Fig. 4: Acoustic signal with the optimized filtering routines of a U-doped SDD at 9°C (3g of active mass).

Given this, the straightforward extra routines to account for identification of the events were put into practice. Figure 5 displays the results of the full implementation of these new acoustic analysis methods for particle identification with α doped SDDs with substantial reduced droplet sizes.

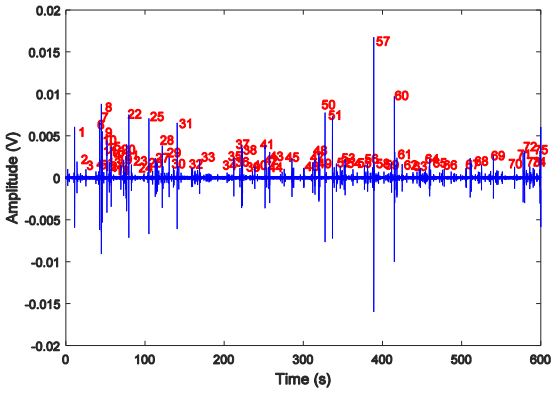

Fig. 5: Identification of the bulk acoustic signals of the particle induced nucleation events.

After the implementation of the new/adjusted identification and validation routines, 75 nucleation events were accounted for. A factor ~2 increase of identification of nucleation events was attained. These results permit improved n - α calibrations for the purpose of particle discrimination when varying fabrication protocols of the SDDs for different uses of these detectors [22], such as detection of alpha particle contamination on ultra low activity-grade integrated circuits.

6 Conclusions

We have been able to successfully create an acoustic bubble nucleation detector which indirectly measures the mechanical energy associated with the event and from this information to selectively discard spurious noise.

The performance demonstrates better than a factor 40 reduction in noise and an extra factor 10 reduction with the filtering application. The lowering of noise and discovery of low signal amplitudes by the acoustic instrumentation and acoustic analysis permits a capability of discriminating nucleation events from acoustic backgrounds and identifying radiation sources. Having an efficiency of 97% at a 95% confidence level on identifying and counting events in substantial data sets like in calibrations.

Further work is actively being pursued to complement these developments of correctly identify nucleation events. For this purpose, the experimental setup is somewhat different, using four microphones outside the vial and one inside (spatially-locating the bubble nucleation and correlating that information with the time interval of events, their relative phase information and time constant at each microphone) [23].

This work is supported by C^2TN/IST and by grants PTDC/FIS/115733/2009, PTDC/FIS/121130/2010, PTDC/EEI-ELC/2468/2014 and IF/00628/2012/CP0171/CT0008. C^2TN/IST authors gratefully acknowledge the FCT support through the UID/Multi/04349/2013 project. The activity of M. Felizardo is supported by FCT grant SFRH/BPD/94028/2013.

References

1. R. E. Apfel. Nucl. Instr. Meth. Physics Research A 162, 603-608, (1979)
2. H. Ing. & H. C. Birnboim. Nucl. Tracks Radiat. Meas., 8 (1-4), 285-288, (1984)
3. International Commission on Radiation Units and Measurements (ICRU). Determination of operational dose equivalent quantities for neutrons. ICRU Report 66. Ashford Kent. UK: Nuclear Technology Publishing. (2001)
4. International Organization for Standardization (ISO). Passive personal neutron dosimetry systems. Performance and test requirements. (in preparation) ISO/TC85/SC2/WG7.
5. F. d'Errico. Nucl. Instr. Meth. Physics Research B 184, 229-254, (2001)
6. F. d'Errico. W. G. Alberts. G. Curzio. S. Guldbakke. H. Kluge and M. Matzke. Radiat. Prot. Dosim. 61 (1-3), 159-162, (1995)
7. H. W. Bonin, G. R. Desnoyers and T. Cousins: Radiat. Prot. Dosim. 46 (4), 265-271, (2001)
8. F. Giuliani, TA Girard, et al. arXiv: hep-ex/0504022, (2004)

9. S. Archambault, F. Aubin, et al. New J. Phys. 13, 043006 (2011)
10. S. Seth and M. Das, Nucl. Instr. Meth. Physics Research A 837, 92-98, (2016)
11. S. Seth and M. Das, JINST 11, nº04, P04015, (2016)
12. M. Felizardo et. al. Nucl. Instr. & Meth. Physics Research A 614, 278-286, (2010)
13. A. C. Fernandes et. al. Astroparticle Physics, 76, 48-60, (2016)
14. A. C. Fernandes et. al. Nucl. Instr. & Meth. Physics Research A 623, 960-967, (2010)
15. M. Felizardo, et al. Phys. Rev. Lett. 108, 201302 (2012)
16. M. Felizardo, et al. Phys. Rev. D 89, 072013 (2014)
17. M. Felizardo, R.C. Martins, et al. Nucl. Instr. Meth. Physics Research A, 585, 61-68, (2008)
18. M. Felizardo, R.C. Martins, et al. Nucl. Instr. Meth. Physics Research A, 589 72-84, (2008)
19. F. Giuliani, C. Oliveira, J.I. Collar, et al. Nucl. Instr. Meth. Physics Research A 526, 348-358, (2004)
20. V. Leroy et al. J. Acoust. Soc. Am. 123 (4), (2008)
21. M. Kafesaki et al. Phys. Rev. Lett. 84, 5919 (2000)
22. M. Felizardo, et al. Nucl. Instr. & Meth. Physics Research A 863, 62-73, (2017)
23. M. Felizardo, R. C. Martins, T. A Girard, et al. Nucl. Instr. & Meth. Physics Research A 599, 93-99, (2009)